SAND2019-2758B

Low-Pressure Dynamic Compression Response of Porous Materials

Tracy J. Vogler and D. Anthony Fredenburg

1 Introduction

The removal of porosity at high rates of strain causes unique phenomena to occur during the dynamic loading of porous materials with respect to their solid counterparts. Most notably, the removal of porosity can generate very high temperatures that can result in the onset of melting or other solid-solid phase transitions to occur at impact conditions much lower than those required for initially solid materials [1, 2]. Under these strong impact conditions, the material response is largely controlled by the equation of state, details of which are discussed in the chapter by Sjstrom. At more modest impact conditions where stresses in the porous material are of similar order as the strength of the underlying solid, the processes involved in the removal of porosity become critical, and both intrinsic and extrinsic properties of the starting material can have an effect on the dynamic response.

The mechanisms involved with the removal of porosity depend on the material, stress level, and strain rate. Nesterenko [3] divided the loading experienced by porous materials into quasistatic and dynamic regimes. In the quasistatic regime changes in the underlying structure of the material are relatively small for metals, while for higher strength brittle materials the structure may undergo significant fracture and fragmentation. Further, under quasistatic conditions the time scales of loading are long enough that particle rearrangement can occur, resulting in the filling of voids with relatively little deformation of the particles. In the dynamic regime, the time scale of loading is much shorter such that both low and high strength materials undergo "substantial morphological" changes from their initial state. Because particle rearrangement does not occur, the removal of porosity must be accommodated solely by deformation and/or fracture of the underlying material. Under these condi-

Tracy J. Vogler
Sandia National Laboratories, Livermore, California, USA, e-mail: tjvogle@sandia.gov

D. Anthony Fredenburg
Los Alamos National Laboratory, Los Alamos, New Mexico, USA e-mail: dafreden@lanl.gov

tions features such as material jets, vortices, and localized melting will occur; these are the characteristic features of porous materials shocked in the dynamic regime. A common feature of shock loaded porous materials is nonuniformity of the material. At pressures where porosity persists, contact points between grains can experience much higher stresses than the bulk, while at higher pressures jetting and related phenomena can cause small regions of much hotter material.

Developing an improved understanding and ability to model the dynamic response of porous materials shocked to moderate stresses (of order of the strength of the underlying material) is critical to many applications. For example, explosive and impact loading is a means by which initially porous materials can be consolidated to nearly fully dense bodies while preserving specific features of the original microstructure not possible by more conventional high-temperature, high-pressure sintering methods [4]. For mixtures of materials specifically designed to undergo exothermic reactions under shock loading (e.g. explosives, thermites), the extent to which energy is consumed and distributed amongst the component materials during compaction is key to determining the onset of the reaction threshold (see chapter by Peieris and Bolden-Frazier). Further, even under the extreme impact conditions imparted by very high energy inputs such as shaped charges, buried explosives, and hypervelocity planetary impacts (see chapter by Collins et al.), the evolution of wave propagation over finite distances dictates that regions exist some distance away from the primary impact zone that will experience moderate dynamic stresses and, thus, must be characterized if a full system modeling approach is required.

However, the measurement and interpretation of experimental results and the subsequent calibration and validation of models at moderate dynamic stresses presents a unique set of challenges. Specifically, at these stresses the measured experimental response includes contributions from the removal of porosity, the deformation and/or fracture of the constituent material, as well as the equation of state. In addition, heterogeneity in the underlying material brings the standard assumptions of equilibrium behind the shock front into question. It is with these and other challenges in mind that the present chapter is framed. Presented first is an overview of the experimental techniques, diagnostics, and resultant uncertainties that are typical when studying the dynamic material response at moderate stresses. Next, the principle approaches for modeling the behavior of porous materials at the continuum and mesoscale levels are given. Having covered the fundamentals of experimental and modeling techniques, the chapter continues with a discussion of several aspects of the dynamic response of porous materials that are observed specifically in the moderate stress regime. To conclude, the authors provide their thoughts regarding several topics that remain outstanding, such that progress in these areas could significantly advance the state of the art in our understanding and ability to interpret and model the response of initially porous materials under moderate shock loading.

2 Experimental Techniques Applied to Compaction

A number of different dynamic loading platforms and diagnostic configurations have been utilized over the years to measure the response of porous materials at moderate stresses. While laser and pulsed power platforms have been added to more traditional gas guns and explosive drives, the diagnostics used to measure the shock consolidation response have also evolved. This section focuses on modern experimental techniques for obtaining the shock Hugoniot of porous materials in the compaction regime. First, details of the canonical experiment used to measure the shock Hugoniot response is given. Next, details relevant to preparing and accurately characterizing competent, loose, and pressed porous bodies are presented. This is followed by a discussion of the instrumentation used to measure characteristics of the shock state. Uncertainties associated with the experimental and diagnostic techniques are presented next. Finally, this section concludes with a brief look at alternate experimental techniques that can be used to characterize the dynamic response of porous materials under more complex loading conditions.

2.1 The Canonical Experiment

Although specific details vary, most planar shock experiments on porous materials take the form of the canonical experiment sketched in Fig. 1. Input is provided by a flyer plate launched by a gas gun or by other means such as an explosive or magnetic drive. The flyer impacts the target at a known velocity, driving a shock wave directly into the sample material or first into a driver layer, as shown in Fig. 1. In most instances the flyer plate and driver plate (if used) are composed of a known material whose shock response is well characterized. The experiment is further diagnosed with time of arrival measurements (gauges, pins, velocity interferometry, etc.) on the planes corresponding to the impact and rear surfaces of the sample to measure the transit time of the shock through the material. In addition, a backing window is often used on both competent and loose samples to facilitate velocity interferometry and to help contain the material during the experiment. For highly competent porous samples a reverse ballistic impact configuration may be used, where the target material is mounted into the projectile and impacted into a stationary window or witness material. Given the relatively high accelerations imparted to projectiles during launch, care must be taken in reverse ballistic configurations to ensure that projectile launch does not crush or otherwise modify the initial state of the sample material.

Target designs for loose or pressed granular samples must incorporate a cell or other containment vessel to ensure the sample dimensions can be measured and maintained from target loading to execution of the experiment. An example of a containment geometry designed specifically for loose, or tap density granular samples is illustrated in Fig. 1b, where the granular material is loaded into the two-step target through single or multiple fill-holes. Studies involving both two- [5] and five-

step [6] targets have been performed. In the design shown in Fig. 1b, the cell serves as both a containment vessel as well as a transparent window for velocity interferometry. Alternate designs consisting of samples at a single thickness (one-step) are also used and are well-suited for granular samples that require some amount of precompression. In these instances the containment vessel, or cell, can be integral to, or separate from the window material. Both the single and multi-step target configurations each come with their own set of advantages and limitations, such that a combination of these two designs is likely required to fully characterize the range of initial conditions achievable for a given material. In either design, the primary *in situ* measurement is time of arrival at the impact and rear surfaces, similar to the measurements performed for competent target materials.

2.2 Samples

Similar to high-precision dynamic studies on solid bodies, initial characterization and sample preparation is critical for obtaining the highest fidelity measurements on porous materials. To this end, the most important characteristics to be considered are accurate metrology, homogeneity within a given sample, and consistency between samples for multiple measurements along the Hugoniot. For competent porous bodies where target samples can be fabricated specifically, or removed from a larger body, such as foams, additively-manufactured trusses, and other porous solids, relatively straight-forward machining methods can be used to obtain the desired sample size and shape. Furthermore, the ability to move, rotate, and inspect all surfaces of a competent body facilitates full metrological characterization. For the canonical ex-

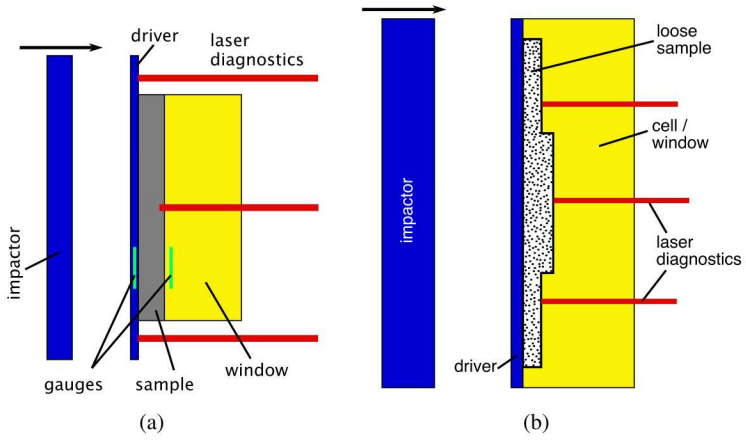

Fig. 1 Schematic of the canonical experiment for (a) competent porous solids and (b) loose or tap density powder samples.

periment discussed in Sec. 2.1, accurate characterization of the sample dimension in the direction of shock propagation is the most important, where tolerances similar to solids can be achieved for competent porous bodies.

Loose or pressed granular materials present additional challenges in initial sample preparation and characterization. For a shock experiment, the powder is typically contained in a cell made of plastic or metal, such as PMMA or aluminum. Metrology is first performed on the cell components, such that the empty cavity volume is accurately characterized prior to powder filling. Filling the fixed volume with a known mass of powder can be done by simply pouring in the powdered material, or by using a combination of pouring and agitation/tapping for a more uniform sample. Such an approach is generally acceptable for particles that are 10s to 100s of microns in size and have relatively simple geometries. As particle sizes are reduced to less than 1 micron, electrostatic forces between the particles can cause clustering and agglomeration between particles, leading to a decrease in the flowability and sample uniformity. Spherical particles tend to have improved flowability during agitation/tapping, but block-like particles have also been found to work well [5–8]. Packing fractions for tapped samples are typically in the range of 20-50%, but higher values can be achieved using specific particle size distributions, e.g. bi-modal or tri-modal [9]. Unfortunately, while there are a number of techniques for testing the flowability of powders for industrial scales, there is not an equivalent approach for quantitatively characterizing similar processes for the small amounts of powder typically associated with shock experiments.

An alternate approach to pouring and tapping is to press the powder to a higher density, allowing for a much broader range of achievable densities. Depending upon the powder morphology and strength, initial densities from just above the pour density to those approaching the crystalline density can be achieved. The upper limit on densities achieved by this method is typically governed by the size of the available press or the need to avoid deforming the cell hardware in which the powder is pressed. In some target designs, it may be necessary to press into a cell containing a transparent window for velocity interferometry (discussed in the next section). In these instances only high strength window materials, such as single crystal sapphire or quartz, can be used during pressing. Other common window materials, such as lithium fluoride (LiF) and PMMA, cannot be subjected to the high stresses during pressing as LiF is prone to fracture under loading and PMMA will deform plastically. If these latter two window are to be used in a target configuration requiring pressing, they must be inserted into the target after pressing is complete. Following completion of the pressing process, an accurate determination of the sample volume must be undertaken. If the compact density is high enough, metrology can be performed directly on the pressed surface and target [10]. However, for lower initial density samples or for relatively ductile materials it may be necessary to use a buffer material of known thickness between the powder surface and the tip of the metrology probe to ensure that the probe itself does not modify the target surface.

Sample homogeneity is also important for accurate determination of the porous compaction Hugoniot. If heterogeneities in the target sample are measured using computed tomography or other through-sample imaging techniques, they must be

accounted for in any analysis of the experiment, or mitigated against by ensuring experimental diagnostics are located away from the heterogeneities. Further consideration must also be given to the spatial dimensions of the underlying pore or solid component with respect to those of the target and diagnostic, such that the target geometry should be large with respect to underlying sample features, and the features should be small in comparison with any diagnostic probe. Regarding target size, mesoscale simulations investigating the propagation of shock waves for different particle configurations have shown evolution in wave propagation characteristics near the impact face as well as non-uniformity in the shock front of order several particles thick [11, 12]. As such, sample sizes should be maximized in the direction of shock propagation to minimize the effects of heterogeneities in the underlying features and for steady shock waves to develop. Furthermore, particle-level simulations on dry sand have shown that significant deviations from the measured bulk wave profile can exist if the spot size of the diagnostic probe is comparable to, or smaller than the underlying features of the porous material. [13] This effect is shown in Fig. 2, where simulated diagnostic probes in the form of tracer particles shown by the light gray lines measure a wide variety of propagated wave profiles, while the tracer average response possesses a shape characteristic of the bulk experimental measurement, but significantly offset in time. If sample or diagnostic probe sizes are such that the underlying microstructural features are expected to influence the experimental measurements, direct numerical simulation approaches should be used to better interpret any measured result.

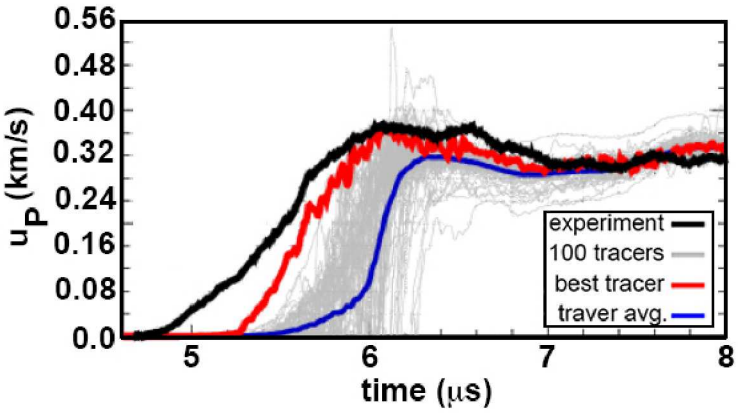

Fig. 2 Propagated material velocity profile measured using VISAR at the window interface for a sand sample impacted at 0.413 mm/μs, compared against simulated wave profiles from 100 tracer particles. The "best tracer" is the one that provides the best agreement with the experimental data. Image adapted from [13].

At a spatial scale larger than that of an individual grain or pore, homogeneity of the sample density within and across the target is also an important consideration.

Sample preparation techniques discussed above can only provide measurements of the bulk geometric density, and depending on the characteristics of the porous material or loading process, significant heterogeneities in local densities can exist. For example, agitation of a loose granular material with a bi-modal particle size distribution can lead to the well-known Brazil nut effect, in which larger particles accumulate at the top and smaller particles accumulate at the bottom, leaving an inhomogeneous void distribution across the sample thickness [14]. This can be especially pronounced for a mixture of two distinct particle species of differing densities. More complicated non-uniformities can also arise in loose and pressed samples such as faults, voids, and tunnels. In instances where limited diagnostic probes are used to measure the shock velocity through a porous sample, the presence of these features can cause difficulty in interpreting the measurements as local density heterogeneities near the diagnostic probe may result in transit times not representative of the bulk. In an effort to characterize features of the initial microstructure and understand how their presence affects shock wave propagation, scientists have begun using radiography and computed tomography to image the initial sample heterogeneities and link those heterogeneities to features of the measured wave profiles. However, this is not yet a routine aspect of experiments, in part because the cell containing the powder can sometimes negatively interfere with the x-ray penetration.

Aspect ratios of the porous targets are also important, and while these considerations are not unique to porous samples, the relatively low wave speeds often found in porous samples requires that particular care must be taken when designing experiments. For experiments where the porous material is surrounded by a cell, window, or baseplate of higher impedance, the sample diameter to thickness ratio must be sufficiently large that edge waves from the surrounding cell or Raleigh waves at the rear powder/window interface do not pollute the shock diagnostic prior to the primary measurement. As a rule of thumb, a diameter to thickness ratio of 10:1 is desirable; however, even this may not be sufficient for highly distended samples. If some information is known about the shock response of the material a priori, computational simulations can be used better understand the limiting aspect ratio for a particular experimental configuration.

The final sample consideration is atmosphere. To the authors knowledge, there have been no detailed studies on the role of atmosphere in the low-pressure shock response of porous materials. Elliot and Staudhammer [15] examined the role of atmosphere on consolidation of stainless steel powders and found that increasing atmosphere from one or 100 atmospheres (1 atm is approximately $1x10^5$ Pa), consolidation of the part was inhibited somewhat. Indeed, in shock consolidation one typically evacuates the sample, but there is no general consensus on the evacuation of the target material in an experiment intended to measure material response. For a material with open porosity, the sample can be evacuated simultaneously with the target chamber by means of a vent or other opening. For closed porosity samples, or those whose pores are filled with a specific gas or liquid, the sample must be robustly sealed to avoid spurious interactions from the surrounding evacuated target chamber.

2.3 Instrumentation

Investigations focusing on the shock compaction region for initially porous materials typically occur at impact velocities up to 1 - 2 km/s and stresses less than several 10s of GPa. As such, some of the instrumentation required to diagnose these experiments have unique considerations with respect to similar experiments conducted at higher impact velocities and stresses. In the canonical experiment (see Fig. 1), impact velocities less then $\sim$1 km/s can be measured quite accurately using a series of shorting pins or laser interrupts. As impact velocity is increased, uncertainties associated with these methods increase, such that optical velocimetry measurements of the accelerated projectile offers more accurate measurements of the impact velocity.

Characterization of the impactor tilt in porous experiments is typically obtained using shorting pins to measure the angle of the impacting projectile directly or optical velocimetry to measure the difference in jump-off times at the rear surface of the drive plate, as shown in Fig. 1(a). Assuming planarity of the impactor, which can usually be readily obtained by the use of relatively thick impactors at the modest velocities associated with compaction, measurements of the impactor tilt allow for arrival times of the shock entering the target to be determined at the spatial locations corresponding to the propagated velocimetry probes, a key component for obtaining accurate shock velocities. For a more in-depth discussion of methods used to characterize impact velocity, tilt, and bow for porous materials, see Fredenburg et al [10].

Following impact, the Hugoniot state in a one dimensional loading experiment is most commonly determined by measuring the shock velocity, U_S, and longitudinal stress, σ. Combined with an inferred material velocity, u_P, from impedance matching [16] and a measured initial porous density, ρ_{00}, the conservation of momentum across a shock discontinuity, $\sigma = \rho_{00} U_S u_P$ (for a material initially at rest), allows one to solve for the remaining unknown. The full thermodynamic state of the material is further determined by applying the conservation equations for mass and energy. Therefore, accuracy for a calculated Hugoniot state depends largely on how well one can characterize the initial density, material velocity and shock velocity or stress for a given experiment. Modern investigations for determining the shock velocity and stress in porous bodies largely employ optical velocimetry and gauge techniques, respectively. Of the gauge techniques, manganin [17] and polyvinylidene fluoride [18] gauges are the most prevalent, while the VISAR [19] and heterodyne / photon doppler velocimetry (PDV) [20] methods are the most common velocimetry techniques.

A schematic illustrating the gauge and velocimetry techniques, along with representative time-resolved outputs for each are given in Fig. 3. One can see that the two techniques differ in the spatial location of their probes. In gauged experiments the primary diagnostic is the impact gauge, which must further be contained within a protective layer, or buffer, typically of similar shock impedance to the gauge itself. The protective layer shields the gauge from the high temperatures associated with void collapse and the heterogeneous nature of the compaction shock (see Eakins and Thadhani [21]) that may otherwise cause degradation or failure of the gauge.

The impact gauge package configuration permits direct measurements of the shock stress in the gauge prior to impacting the sample, σ_{gi}, as well as the stress in the sample as it is reflected back into the impact gauge, σ_{sH}. Placement of a second gauge behind the sample further allows for a direct measurement of the stress associated with the second shock or release, σ_{sr}. Shock transit times through the porous target, Δt_S, can also be measured using the combined impact/rear gauge package method; however, calculation of shock velocities using this technique must take into account the thickness of the gauge package and protective layers. With gauge package and buffer thicknesses on the order of several millimeters, shock velocities in agreement with impedance matched values have been demonstrated for silica powders of varying initial density after accounting for the gauge package thickness [22], while for much thinner gauge packages agreement has been demonstrated without correction for a system of nano-sized iron powders by [23].

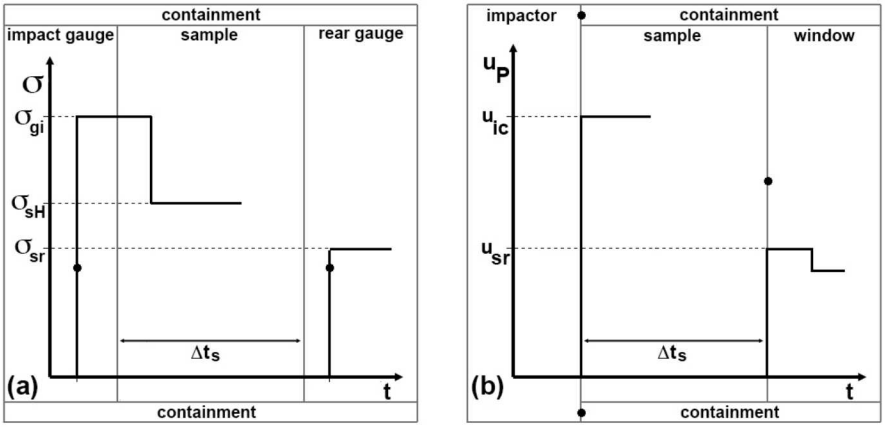

Fig. 3 Schematic illustrating the (gray) experimental configurations for (a) gauge and (b) optical velocimetry diagnosed experiments. Representative wave profiles taken at the spatial position indicated with • are overlain to provide perspective on differences in timing between the two techniques. In this configuration impact occurs from left to right.

In contrast to gauged experiments, those diagnosed using optical velocimetry directly measure the shock transit time through the sample. Depending on the geometry of the target, velocimetry measurements at the impact plane can provide full characterization of the input shockwave profile, measurements of shock arrival time only, or some combination of the two. For example, if the containment shown in Fig. 3 is composed of an optically transparent material, the velocity history at the impactor/containment interface can provide a direct measurement of the input shockwave profile. However, in target configurations where the containment (see Fig. 3) is not optically transparent, velocimetry at the impact plane is typically a free surface velocity measurement of the impactor, which may or may not contain information other than shock jump-off times. Evaluating the velocity history entering the porous material is important at the low-to-moderate stresses relevant to

compaction because many of the standards used to construct the experimental target fixtures exhibit non-steady wave characteristics in this regime. For example, powder targets pressed *in situ* require an impactor with moderate strength to support the loads applied during the pressing operation. Thus, impactors in this configuration may be composed of metals such as aluminum or copper which can exhibit two wave structures under shock loading due to elastic-plastic transitions [24], or iron containing steels which can exhibit similar wave structures due to phase transformations [25]. Therefore, care must be taken in the experimental design to ensure that a planar steady wave is imparted into the target material when applying the Rankine-Hugoniot jump conditions.

Velocimetry measured at the rear, or propagated, surface of the target sample provides a measure of the shock transit time as well as insight into the physical mechanisms of compaction. For example, the amount of temporal dispersion in a propagated velocity history can be linked with the dissipative nature of the material being shocked, as shown in Fig. 4(a). In this comparison sand and CeO_2 powders at similar initial percentages of their theoretical maximum densities (% TMD) are shock loaded and produce very different propagated wave profiles. For sand, the shock rise time spans several hundred nanoseconds with significant curvature at both low and high material velocities, while that for CeO_2 exhibits a sharp rise over several nanoseconds followed by curvature as the velocity approaches its maximum. For the two experiments in Fig. 4(a), differences in the theoretical density, particle size, and Hugoniot stress (Sand/CeO_2; ρ_0 = 2.6/7.2 g/cm^3, Φ = 200/7 μm, σ_H = 0.8/1.8 GPa) make it difficult to link specific features of the initial and shocked states to the dispersion measured in the wave profiles. However, regardless of its origin, this dispersion must be accounted for when performing an analysis of the Hugoniot state and its corresponding uncertainties. See Section 4.2 for further discussion of the rise time for shocks in porous materials.

When using velocimetry to measure propagated wave profiles, some researchers [5, 6, 26] have used buffers between the measurement plane and the granular sample. This is done to protect the reflective surface, particularly important for VISAR measurements, and to "average out" the velocities so that a single velocity history is obtained. An extreme case of this is that of Winter and McShane (this volume), who used a 6 mm stainless steel witness plate as a buffer to obtain PDV measurements of additively manufactured truss structures with pores of order millimeters in size. In a study on CeO_2 powders, Fredenburg et al [10] measured propagated wave profiles after traveling through an 8 um Al foil in contact with the powder using PDV and after traveling through the foil and a 0.5 mm PMMA buffer using VISAR. Their results are shown in Fig. 4(b), where both profiles are observed to display similar characteristics in the initial rise and late time velocity plateau regions. However, in the transition region into the shock plateau, the two methods give different responses, with PDV at the powder/foil interface exhibiting an oscillatory behavior characteristic of its ability to measure multiple velocity fields, and VISAR at the buffer/window interface exhibiting a smooth transition characteristic of PMMA [27].

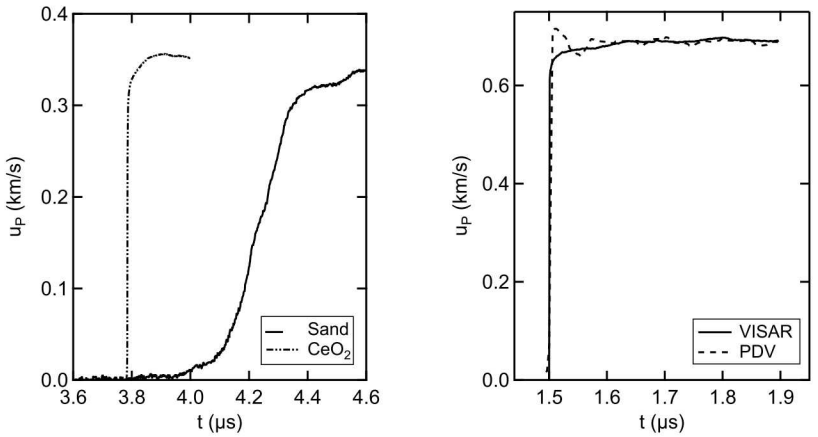

Fig. 4 (a) VISAR transmitted wave profiles for ρ_{00} = 59% TMD sand and ρ_{00} = 55% TMD CeO_2 shocked to ρ = 92% and 79% TMD, respectively, illustrating the variation in shock rise times. (b) Transmitted wave profiles measured from a PDV line-out at the powder rear surface and a VISAR at the buffer/window interface on CeO_2 powder; traces are shifted in time for comparison. Data for sand from Brown et al [5] and from Fredenburg et al [26] for CeO_2.

With sample heterogeneity (material + void) underlying all experiments on porous materials, experimental efforts in recent years have been undertaken to better understand this heterogeneity using spatially-resolved velocimetry as well as advanced x-ray sources. Trott et al [8] used line-VISAR to study the spatially-resolved shock response of pressed sugar, examining heterogeneities in transmitted wave profiles with respect to impact velocity, sample thickness, and particle size distribution. Using similar methods, Baer and Trott [28] investigated the response of ordered stackings of tin spheres. In more recent investigations, synchrotron x-ray sources are being used to probe the heterogeneous nature of shock propagation in porous materials *in situ* (see Jensen et al. chapter). Experimental techniques such as these, when coupled with complimentary mesoscale modeling techniques, offer great promise toward increasing our physical understanding of the particle-level mechanisms active during compaction and further interpretation of the bulk measurements that have been common practice for the past several decades.

2.4 Uncertainty and Error Analysis

In the previous section, much of the discussion of instrumentation was focused on velocimetry techniques for measuring the transit time of a shock through a known initial thickness sample. While knowledge of the shock transit time is useful, the true value of a shock compaction measurement is in being able to determine how

the material responds in the stress-density plane, i.e. how much porosity is removed and densification of the bulk occurs for a given applied stress. Further, a good measurement also strives to have low uncertainties in the calculated quantities of stress and density ($\rho = 1/V$), such that this information may be used to accurately calibrate and/or validate a continuum compaction model (see the next section for more discussion of compaction models).

A transit time measurement can be converted to a point on the stress-density plane using the conservation equations, and it is in these relations where uncertainties are captured. For stress:

$$\sigma = \rho_0 U_S u_P \tag{1}$$

such that uncertainties in the initial density, shock velocity and material velocity contribute proportionally to the total uncertainty in stress. Therefore, a skilled experimentalist will work to design a target fixture and diagnostic suite that reduces the individual uncertainties in ρ_0, U_S, and u_P to keep the uncertainty in stress low. However, the relationship for density:

$$\rho = \rho_0 \frac{U_S}{U_S - u_P} \tag{2}$$

introduces larger uncertainties in the calculated values of density. This is due to the fact that values for the shock and material velocities can be quite similar in the low stress compaction regime. While a requisite for the development of a shock wave is that $U_S > u_P$, if U_S is only slightly larger than u_P then the denominator of Eq. (2) is small, such that even small uncertainties in either the shock or material velocities can result in relatively substantial uncertainties in stress. This is a feature unique to initially porous materials, and imposes real limitations in accurately characterizing the shock compressed density.

While the conservation relations serve as the underlying basis for all uncertainty analyses, several specific methods have been applied to porous materials and are discussed further here. A key work on the analysis of uncertainties for shock experiments performed on solid materials is that of Mitchell and Nellis [29]. They considered both random uncorrelated uncertainties and systematic uncertainties to estimate the total uncertainties in both the measured and calculated Hugoniot state values. This approach was applied to porous granular materials by Fredenburg et al [10], who noted that the assumption of sample homogeneity in the initial density state is likely not as strictly enforced for porous materials as it is for solids. As such, the authors acknowledge the presence of inhomogeneities in granular samples and suggest tomography as a potential means to characterize sample heterogeneities prior to an experiment. However, in the absence of tomography they advocate that multiple measurements of the shock velocity for a given experiment may be able to account for some of the sample heterogeneities in the analysis of experiments.

Recently, Root et al [30] utilized a forward Monte Carlo approach for calculating uncertainties in the high-pressure shocked states of hydrocarbon foams when impedance matching with a known standard is utilized. In this work, the authors too note the presence of sample heterogeneities, but in this case are focused on local

heterogeneities at the scale of the grain/pore. For the foams investigated, which had pore sizes of order 1 μm, they argue that if the transit time of the shock across a pore is less than the temporal resolution of the diagnostic (in this case VISAR), then the shock can be treated as an equilibrium state and the Rankine-Hugoniot jump conditions can be applied. While the Monte Carlo approach has not yet been utilized in published reports on the low-pressure shock response of porous materials, the authors are currently working to extend this approach to that regime.

While both analysis methods are useful in ascribing uncertainties to a single experimental data point, an alternate approach to capturing the uncertainty in the compaction response for a given initial density state is to perform a statistical number of experiments at the same initial conditions of density and impact velocity and evaluate the scatter observed between the points. While the authors know of no studies that have performed of order ten or more repetitions of a single experiment, more limited studies have found that the spread between the Hugoniot states of multiple experiments performed under nominally identical conditions is similar to the uncertainty bounds assigned to any given data point. An example of this behavior is shown in Fig. 5, which shows the spread in the calculated Hugoniot volumes for experiments on sand and copper under nominally similar impact conditions. Inspection of these data sets reinforce the observation that underlying heterogeneities at one or more length scales in porous materials are the principal driver for uncertainties in the Hugoniot state. For a more in-depth study of the role heterogeneities may play in the shock compression response of initially porous materials, one may also look at alternate loading techniques.

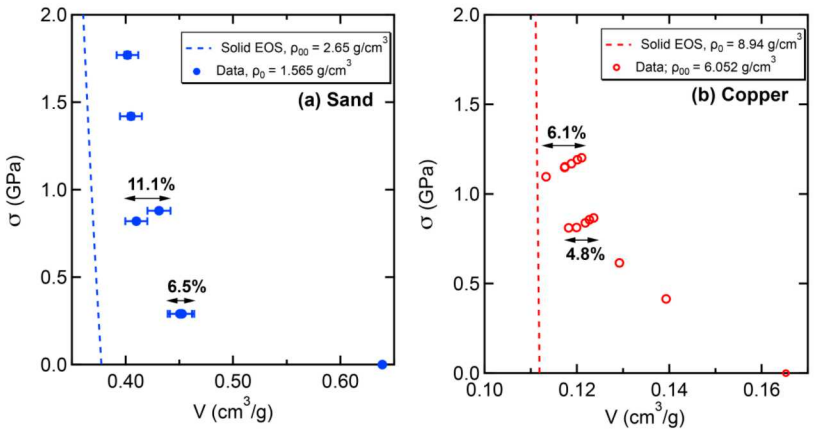

Fig. 5 Compaction data for sand [5] illustrating uncertainties associated with individual data points, and copper [31] illustrating the spread in Hugoniot states for similar initial condition experiments. Percentages are with respect to the ambient solid volume.

2.5 Non-Planar Loading and Alternate Experimental Platforms

The canonical experiment discussed in Section 2.1 is used to measure the response of porous materials under the idealized conditions of one dimensional planar shock loading. As such, application of the conservation equations to these types of experiments yield only the components of stress and strain in the direction of shock propagation. Given the complex nature of shock waves in real-world applications (see chapters by Collins et al., Omidvar et al., and Peiris and Bolden-Frazier), the shock compaction response under multi-dimensional loading must be understood and characterized for the development of accurate models. Over the years, several different approaches have been developed for this purpose, though none have been used extensively.

Of specific interest to the relatively low stress regimes associated with compaction is the ability to measure the deviatoric (shearing) stress response, which allows for characterization of the strength (deviatoric) response under dynamic loading. Tang and Aidun [32] have reviewed the experimental and theoretical aspects of the combined pressure and shear technique, where measurement of the longitudinal and transverse waves are used to study the constitutive properties of solids. These methods have been applied by Sairam and Clifton [33] to granular Al_2O_3, by Vogler et al [34] to sand and granular WC, and by LaJeunesse [35] to sand. The experiments consisted of a thin layer of the granular sample sandwiched between two plates that are intended to remain elastic. Impact is planar but at an angle θ (typically 20-30 degrees) to the direction of projectile motion, which generates both longitudinal and shear waves in the target. The amplitude of the shear transmitted through the sample is taken as a measure of its strength. These studies have shown that the strength of the porous material increases approximately linearly with applied pressure, at least over the range studied. The approach is limited to thin samples, which can be difficult to prepare or non-representative for granular materials. Also, the approach has only been applied to granular materials up to about 3 GPa because of the desire to remain in the elastic regime of the confining plates.

Recently, an approach to examine the evolution of non-planar features in a propagating shock wave [36] has been utilized in an attempt to probe the strength of a shocked porous material [37]. In continuum and mesoscale simulations, increased material strength is found to delay the decay of the perturbation. Thus, it should be possible to fit a strength model for the material of interest to perturbation decay data for varying conditions (impact velocity/pressure, volume fraction, etc.). Only limited results with this technique have been reported to date, but additional work on the technique is ongoing.

While all of the experimental approaches discussed above have been planar or quasi-planar, cylindrical geometries have been used extensively as a consolidation technique [38–41] and to study materials science issues [42, 43]. However, to the author's knowledge there has only been a single reported use of the cylindrical configuration as a means to study the low pressure dynamic response of a porous material [44]. They utilized current pulses through conductive coils to radially compress a copper tube filled with sand. PDV diagnostics on the exterior provided quantitative

(but incomplete) information on the response of the sand. Additional development of this approach is needed before it will be suitable for characterizing porous material response.

3 Computational Techniques Applied to Compaction

The computational approaches applied to simulating dynamic consolidation processes can typically be divided into two classes. The first of which models the porous material as a continuum, which requires homogenization of the solid and void components into a single simulated material. The second of which captures the material at the mesoscale, which includes discreet modeling of both the solid and void components. Both of these approaches offer unique and complimentary capabilities, and are discussed below.

3.1 Continuum Modeling

Using the experimental methods described above, researchers have measured the shock compaction response for a wide variety of materials ranging from relatively soft and ductile metals to hard and brittle ceramics. These data can be further utilized to calibrate or validate continuum-level compaction models used in simulations. Over the years, several different modeling approaches have been developed to capture the continuum-level shock response associated with the removal of porosity. In the first class of models the shock stress is assumed hydrostatic, such that the stress tensor is assumed to be spherical and only the pressure P is considered. In the second, the full stress tensor is considered. An example of the later approach is given in the chapter by Banerjee and Brannon of this book, so only the former approach is covered here.

Hydrostatic compaction models are used widely across the shock physics community due to their relative ease of implementation. Of these models, the most prevalent is the P-α model, originated by Herrmann [45] and expanded upon by Carroll and Holt [46]. In this framework alpha is a measure of the distention, and is defined by $\alpha(P) = V(P)/V_S(P)$, where $V(P)$ is the specific volume of the porous material at pressure P and $V_S(P)$ is the specific volume of the fully solidified material at the same pressure P. In this analysis, shock energies for the solid and porous materials are assumed equivalent at a given pressure and temperature. Therefore, α captures the extent to which the volume of the porous material differs from that of the solid at a given pressure and energy. When $\alpha \to 1$, the porous response coincides with that of the initially porous, but now fully solidified material.

Depending on the type of material and range of initial porosity being captured, the specific formulation for $\alpha(P)$ can take many forms. In much of the early work on metals, see for example Herrmann [45], Butcher and Karnes [47], and Boade

[31], $\alpha(P)$ was separated into elastic and plastic components, where the extent of the elastic region was found to decrease with increasing initial porosity. Due to the relatively small change in volume associated with the low-pressure elastic region, in some instances $\alpha(P)$ in this region can be sufficiently captured by treating it as a constant, equal to its initial value at zero pressure α_0 [48]. In the region of plastic deformation, large volume changes occur due to the removal of porosity, and a discreet functional form must be applied for $\alpha(P)$. A polynomial in terms of P was first suggested by Herrmann [45]:

$$\alpha(P) = \alpha_0 + \alpha_1 P + \alpha_2 P^2 + \alpha_3 P^3 \tag{3}$$

and was found to adequately capture the compaction response of 17-90% initial density porous iron. For other materials, application of Eq. (3) has been unable to sufficiently capture experimental data, see for example Borg et al [22] and Fredenburg and Thadhani [49], so alternate representations for $\alpha(P)$ have been developed. Other functionals for $\alpha(P)$ such as the exponential [50]:

$$\alpha(P) = 1 + (\alpha_E - 1)e^{-\hat{a}(P-P_E)} \tag{4}$$

and power-law [5]:

$$\alpha(P) = \left(\frac{P_S}{P}\right)^{1/n} \tag{5}$$

forms have been proposed to provide alternate relations for empirically fitting experimental compaction data. In Eqns. (4) and (5) the subscript E corresponds to values of α and P at the transition from the elastic to plastic region and $\hat{a}$, P_S, and n are empirically-derived fitting parameters.

In compliment to the P-α model, the P-λ model has also been developed to capture the evolution of porosity under dynamic loading [51, 52]. In this formulation, λ is the progress variable for porosity evolution and takes the form:

$$\lambda(P) = 1 - e^{-(P_l/Y_l)^n}, \tag{6}$$

where Y_l and n are empirical fitting parameters with the former having units of pressure. In this model, the specific volume of the initially porous material is defined as a mixture of the material in its equilibrium equation of state response and in a non-equilibrium elastic response, evolved through $\lambda(P)$. This formulation has been used successfully to capture the low-pressure compaction response in a wide range of both homogeneous and heterogeneous materials [5, 49, 53]. An example from Fredenburg and Thadhani [49] showing the variation in P-α and P-λ model fits with compaction data from a powder mixture of Ti + Si is shown in Fig. 6. Here, the three model forms that fit the data well have empirically derived fitting parameters, while the fourth fit, which shows the largest disagreement with the data, does not include any free fitting parameters. Rather, this fit relies entirely on the static yield strength of the mixture to predict the compaction response.

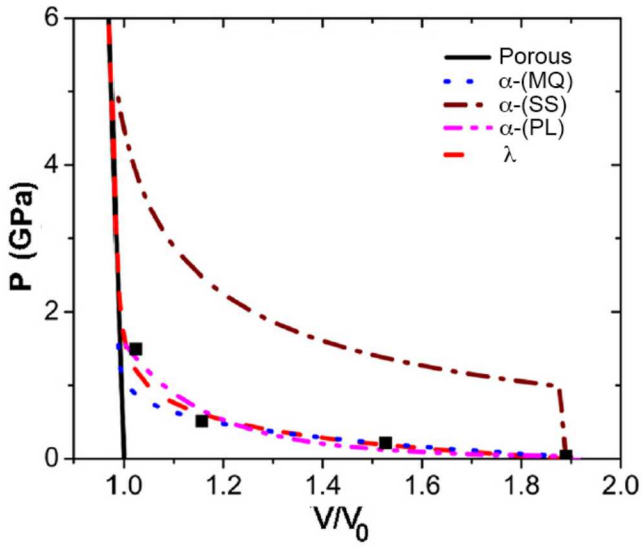

Fig. 6 Shock compaction data for a Ti + Si powder mixture plotted against four distinct continuum model formulations, where α and λ in the legend indicate that a P-α or P-λ model was used in the fit. Details of the functional forms are: (MQ) = $\alpha(P) = 1 + (\alpha_E - 1)\left(\frac{P_S - P}{P_S - P_E}\right)^N$; (SS) = $\alpha(P) = \frac{1}{1-e^{-3P/2Y}}$; (PL) = Eq. (5), and λ = Eq. (6). Image adapted from [49].

In more recent years, Collins et al [54] extended the $\varepsilon - \alpha$ [55] model to include data for highly porous initial states. In this model α is again the progress variable for compaction; however, here distention is evolved using knowledge of the volume strain, $\alpha(\varepsilon)$ rather than the pressure as it is for the P-α model. By advancing distention using volume strain, the $\varepsilon - \alpha$ model allows for increased computational efficiencies in certain hydrocode implementations that would otherwise require simultaneous solution of both the pressure and distention through iterative means. Similar to the models above, the removal of porosity is separated into elastic and plastic regions, and $\alpha \to 1$ when all porosity is removed. While general in its form, application of this model has been largely focused on simulating high-velocity impacts of planetary bodies, see for example Bland et al [56] and Davison et al [57].

Each of the three models discussed above are applied similarly in that they require an existing data set to determine optimal values for their empirically-derived fitting parameters. Further, all have limited utility in predicting the compaction response for a material and/or initial condition outside of the range for which the model was calibrated. As such, development of a predictive capability for compaction modeling continues to be an active area of research.

3.2 Mesoscale Modeling

Modeling the shock loading of porous materials at the mesoscale, is typically undertaken to provide insight into the phenomenology of material behavior at the grain scale. Porous materials are well-suited to this type of modeling because they inherently possess intermediate length scale features, that of the grains and pores, which can play an important role in material behavior. In the 1997 predecessor to this volume, Benson [58] reviewed mesoscale modeling in great detail. Since that time, mesoscale modeling techniques have matured significantly, driven primarily by a tremendous growth in computing power.

While early mesoscale modeling studies considered primarily planar shock loading configurations involving a small number of particles, increased computing power has led to much larger domains. Currently, it is not uncommon for planar shock simulations to include domains that are comparable to the sample thicknesses commonly used in shock experiments, i.e. a few to several millimeters. In these simulations, rigid or periodic boundary conditions are often imposed on the lateral faces to simulate the uniaxial strain loading of planar shock experiments. As simulation domains have grown, it has also become possible to consider loading configurations other than planar shocks, such as penetration [59, 60], cylindrical loading [61], and perturbation decay [37].

Current computational capabilities have also made possible the study of mesoscale calculations in three-dimensions (3-D), (c.f. [8, 61–63]) though two-dimensional (2-D) calculations are still routinely undertaken due to their much lower computational cost Borg and Vogler [62]. examined the differences in compaction between 2-D and 3-D mesoscale simulations and found that the behavior of WC powder could be accurately simulated with both 2-D and 3-D models. However, different treatments of interparticle interactions were required to achieve agreement between the two techniques, and differences in the temperature and energy distributions between the two cases were noted, suggesting that investigations where energetics or reactive materials are of primary concern, it may be best to model these systems in 3-D. Thus, while some problems (such as penetration, see chapter by Omidvar, Bless, and Iskander) are inherently 3-D, it may be possible to model other shock phenomena relatively well in 2-D.

Also in the 1997 predecessor to this volume, Benson [58] laid out an approach for generating random distributions of circles in a 2-D domain for generating initial microstructures, which has been used and adapted by others over the subsequent years [11, 64]. Similar spherical approaches have also been used in more recent 3-D calculations (c.f. [62]). Regarding the generation of synthetic initial microstructures composed of spherical particles, Borg and Vogler [64] examined a number of different aspects of this approach, and emphasized that random arrangements of particles were needed to reduce systematic biases in computational results.

Compaction studies of other 2-D shapes [12, 64] have generally shown that the behavior of inert materials is relatively insensitive to particle shape. However, computational investigations focused on reactive mixtures have shown that shock initiation can be strongly influenced by particle morphology. [21] In studies of explosive

powders and their simulants, Baer [65] and Trott et al [8] used a particle insertion approach to generate realistic arrangements of cubes, while other researchers [66, 67] have imported real experimental microstructures from cross-sections of porous samples to generate complex 2-D domains, primarily for reactive mixtures.

In most mesoscale modeling studies of granular systems, relatively simple constitutive models are used to describe the solid particles. For metals and polymers, material behavior is commonly captured using an equation of state and metal plasticity models to capture the hydrostatic and deviatoric response under shock loading. It is also common practice to model brittle materials in the same fashion, even though fracturing of the constituent particles most likely occurs. This simplification is undertaken largely due to the difficulty in treating fracture in mesoscale simulations, particularly since fracture can quickly drive particle size below the resolution limit of the initial simulation. Despite this shortcoming, there has been some success at matching observed bulk behaviors with mesoscale models that employ these simplified techniques [11, 63].

The execution of mesoscale simulations focused on the shock loading of granular materials can be conducted using several different frameworks. Of these frameworks, the Eulerian, Lagrangian, and molecular dynamics approaches are discussed briefly here. In the Eulerian approach, which is composed of a fixed computational grid through which material moves, hydrocodes such as CTH [68], iSale [55], and others have been used to study the shock and impact response of granular and porous systems Benson [58], indicates that the first such study using the Eularian framework was performed by Williamson [69], with numerous other studies to follow [11, 58, 59, 61–64, 70, 71]. This framework is particularly well suited to the consolidation of porous systems because of its ability to easily handle large material deformations. However, this approach is less robust for simulations where fracture and interfacial interactions are an important component of the system being investigated, as models of this type are not well suited for Eularian codes. Despite these limitations, to date, most mesoscale studies of shock-loaded porous materials have undertaken using Eularian methods.

In addition to the Eularian framework, studies of granular systems have also been undertaken using Lagrangian finite element method (FEM) approaches, [60, 72, 73] where the mesh elements move with the material when deformation occurs. This structure has restricted the use of FEM for mesoscale simulations at high strain-rates (where large deformations are expected to occur), because large deformations can cause mesh entanglement. In instances where large deformations are expected to occur, Lagrangian methods can be evolved without mesh entanglement using ALE (arbitrary Lagrangian Eularian) techniques, where remapping of highly strained elements occurs and allows for material to flow through the elements as they do in Eularian simulations. This re-mapping is typically performed locally, near the regions of highest deformation, and require accurate material advection models that are not usually developed for Lagrangian-only frameworks. In addition to facing challenges with respect to large deformations, Lagrangian frameworks are also not currently well suited for granular fracture, though general advancements in cohesive

zone algorithms are allowing for fracture to be modeled in Lagrangian codes more readily. [74]

Lastly, classical molecular dynamics has found use in simulating the shock response of porous materials because it has the distinct advantage of explicitly treating all aspects of material behavior, including fracture and plastic deformation, at least to the accuracy of the interatomic potential used. While some nanofoams [75] and metal organic frameworks (MOF's) [76] have been accurately represented in MD simulations, it is impossible to represent the experimental microstructures of most porous materials with today's computational capabilities. Instead, simulations must be conducted at length and time scales that are much smaller than those of real shock experiments [77, 78]. However, there are some indications that even simulations at such a disparate scale can still reproduce some aspects of the bulk response. While computational capabilities continue to improve and simulations of larger domains will soon become possible, it will likely still be many years before simulations with length scales of millimeters and time scales of microseconds can be performed using classical molecular dynamics. For a more thorough discussion of this technique, see the chapter by Lane in this volume.

4 Phenomenology

Having covered details of the experimental methods by which Hugoniot data in the compaction region is obtained (Sec. 2), and the theoretical methods by which this data are captured in computational models (Sec. 3 and the chapter from Banerjee and Brannon), the focus now shifts toward some of the unique behaviors observed during the compaction of initially porous materials. It should be noted that in most of the instances discussed, it is required to have rather large data sets for individual material systems or across different material systems to make these comparisons. As such, the authors acknowledge the important role that comprehensive studies on porous materials play in advancing our understanding of these unique phenomenologies.

4.1 Shock Precursors

In competent porous materials, separation between an elastic precursor and the bulk shock wave is commonly observed at low to modest stresses, in a manner similar to fully-dense solids. In these systems the precursor amplitude, referred to at the Hugoniot elastic limit (HEL), has been observed to decrease with increasing porosity. For example, Butcher and Karnes [47] found a linear log-log dependence of the yield point with initial density in sintered iron specimens with $\rho_{00} > 60\%$ TMD, while Brar et al [79] showed a linear reduction in the HEL with initial porosity in boron carbide sintered to densities greater than 83% TMD. Additively manufactured truss

structures studied by Winter and McShane (see chapter in this book) also exhibited elastic precursors under impact loading, though their study only focused on a single initial fractional density of 64% TMD. In these and other investigations on competent porous bodies, the presence and magnitude of the elastic precursor tends to be more likely at low to moderate levels of initial porosity.

In systems composed of loose or pressed granular materials, elastic precursors in transmitted stress or velocity profiles are not typically observed due to the dispersive nature of the initial configuration. However, Neal et al [80] observed substantial precursors in shock loaded mono-disperse spherical glass beads at low stresses, which became overdriven and disappeared as shock stresses were increased, as shown in Fig. 7. The authors note that the precursor was likely not wholly elastic because it produced substantial densification; rather, it was likely some combination of plastic deformation and particle rearrangement. Lajeunesse et al [63] observed a less pronounced precursor in coarse-grained sand. In pressed granular sugar, Trott et al [8] observed precursor waves using spatially resolved velocimetry techniques, and found the temporal duration of the precursor diminished as impact velocity and applied stress increased. Despite different sample preparations, initial densities for these studies were about 65% of the theoretical maximum density. Other studies investigating the dynamic response of granular WC [6], CeO_2 [26], and sand [5] at approximately 55% TMD have not shown the presence of elastic waves. Taken together with the observations on yielding in competent porous bodies, precursor behavior (whether purely elastic or some combination of other deformation mechanisms) is more prevalent at low impact stresses in systems with low initial porosity levels.

4.2 Shock Rise Time

Heterogeneities at length scales of the grains/pores and also those at larger length scales associated with the bulk give rise to unique wave propagation characteristics in shock loaded porous materials. Evidence of this behavior is most prevalent in the compaction regime, where the applied dynamic loads are not sufficient to overdrive the inter- and intra-granular strength (c.f. Nesterenko [3], Sheffield et al [7], Tong and Ravichandran [81]). Consequently, unique scaling behavior has been observed for initially porous materials that is in stark contrast to solids. In nominally homogeneous solid materials (and some two-phase solids), the strain rate in the shock front scales with stress to the fourth power, $\dot{\varepsilon} \propto \sigma^4$ [82]. This so-called "fourth power law" is widely observed and has become part of the canon for the field of shock physics. However, the introduction of heterogeneity alters this scaling and, in the case of layered materials, has been shown to produce a second power scaling, $\dot{\varepsilon} \propto \sigma^2$ [83]. More recently, experimental wave profiles were examined for tungsten carbide and sand and were found to display a first power scaling, $\dot{\varepsilon} \propto \sigma$ [5, 6].

Vogler et al [84] examined the three power law scalings and were able to identify non-dimensional groups for the second and first power law scalings that allowed

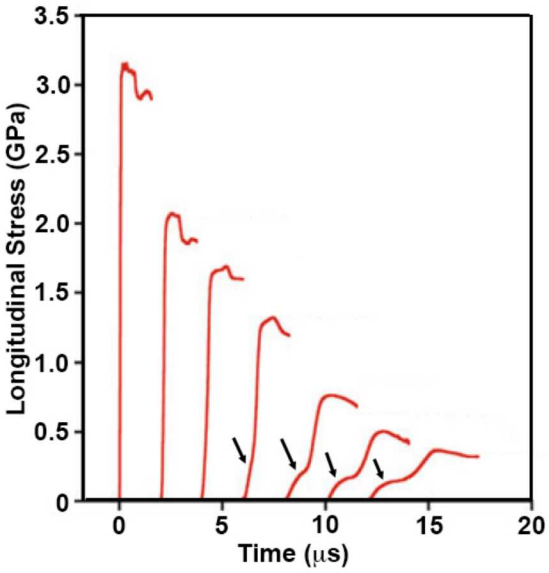

Fig. 7 Evolution of transmitted stress wave profile in spherical glass beads with increasing input stress. Arrows indicate the approximate location of the transition from the initial precursor state to the primary plastic front. Image adapted from Neal et al [80].

for the response of a wide variety of different materials to be collapsed onto a single curve. Results from this analysis are given in Fig. 8, where it is observed that first power law scaling is exhibited by a very broad range of initially porous material types, from porous polymeric foams to high strength granular ceramics such as tungsten carbide and titanium dioxide. Somewhat surprisingly, the best scaling is obtained without inclusion of a strength or hardness for the material.

In addition, Vogler et al [84] proposed a simple conceptual model to explain the first power scaling. The model considers the delay in wave propagation through a series of aligned particles caused by a missing particle. This gap must be closed through motion of the material across the gap, slowing the wave in that region. By relating that delay to a strain rate, they were able to obtain values for the scaling exponent close to unity for reasonable values of the compaction response. Thus, they propose that the mechanism of mass propagation as a means to close voids in the porous material is the essential element in the first-power scaling observed in porous materials. First power scalings observed experimentally for porous materials have also been found in mesoscale computations based on Eulerian hydrocodes [11, 62], though some effect of the method used to estimate the strain rate has been found. Simulations utilizing a particle-based Lagrangian code have also been found to display similar scaling [84].

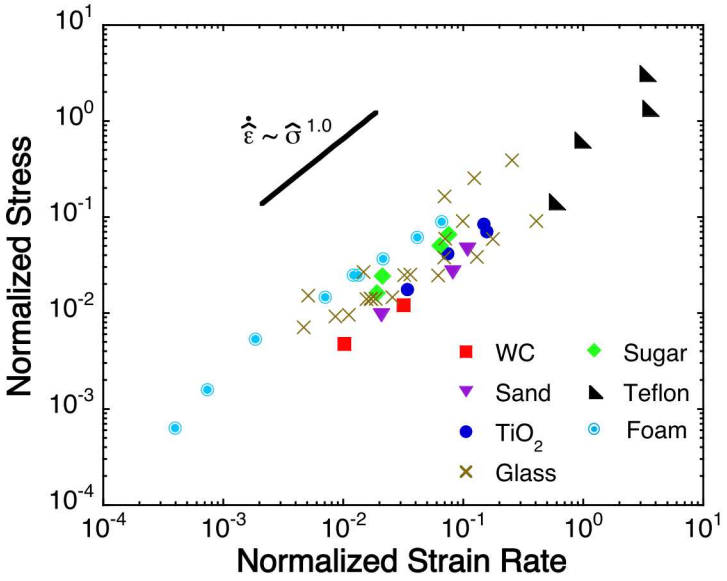

Fig. 8 Normalized stress versus strain rate for shock experiments on a wide range of porous materials showing a first-power scaling relationship. Image adapted from [84].

4.3 Porosity Enhanced Densification

Another interesting phenomenology associated with porous materials is manifested in the interplay between the thermal and mechanical resistances to densification. For materials subjected to strong shocks (well in excess of the stresses required for complete densification), the conservation of mass, momentum, and energy across a shock front predict decreasing levels of densification for increasing levels of initial porosity at an equivalent applied stress. This results in a "family" of porous Hugoniots with increasing displacement from the solid as initial porosity is increased [85], a behavior governed by the increasing thermal energy associated with shock loading higher porosity materials. As initial shock stresses are decreased, the Hugoniot response transitions from being governed by the thermal (and electronic) response of the continuum to one dominated by the mechanical response of the grains and pores.

By definition, a porous material is composed of at least two components, a solid component with relatively high strength and a gas/void component with minimal resistance to shear. Under compression these two materials behave quite differently, such that compression of the gas/void component is favored over that of the solid constituent. Therefore, at relatively high initial porosities there is little resistance to densification, such that large increases in shock compressed densities can be achieved with low stresses applied to the composite material. Conversely, higher stresses are required to achieve significant densification for materials with

low amounts of initial porosity. This is likely one of the contributing factors to the observation of Brown et al [5], who noted that the P-α model formulation developed by Herrmann [45] which contains an elastic response and a plastic response given by Eqn. (3) was unable to fit the data for 59% TMD porous sand. Rather, better agreement was obtained using compaction models that contained exponential and power-law functions and allowed for large initial increases in shock compressed density at low applied loads.

Further evidence of a transition in the compaction response from that which offers little resistance to densification at high initial porosities, i.e a purely plastic response, to a more rigid response that must be captured by distinct elastic and plastic regions as initial porosity is reduced is found in the shock response of tungsten. Figure 9 gives the dynamic response for initially porous tungsten at several initial distentions ranging from 28% to 80% TMD along with representative P-α model fits to each data set using Eqn. (4). For the lower initial densities of tungsten corresponding to 28% and 55% TMD, the compaction response can be captured well using only the plastic response of Eqn. (4). However, as initial density increases the elastic response must be included to achieve sufficient agreement between the data and the model. The data for tungsten, along with that of sand, suggests there is a maximum initial packing fraction at which the compaction response transitions from perfectly plastic to elastic plus plastic for both ductile and brittle materials, and that this transition occurs somewhere between 59% - 66% TMD. It should be noted that the maximum packing fraction for a random packing of spheres is approximately 64% TMD, such that this value might serve as a practical upper limit on the transition for initially porous granular materials. However, further experimental and theoretical work is needed to verify this assumption.

4.4 Morphology Effects

Mesoscale material characteristics such as the size and shape of the solid and void/gas components are important characteristic of porous materials in that they can be measured experimentally prior to the dynamic event. If these intrinsic properties can be further related to particular compaction phenomena, then it may be possible to predict certain features of the compaction response by having only limited information about the material initial state. For example, it has been observed in many granular systems that particle morphology and size distribution influences initial packing fractions, see Sec. 2.2. These properties can affect the preparation of granular samples for dynamic experiments, and may influence shock wave characteristics in those materials, as discussed in Section 4.2. At present, the role of intrinsic property variations on the bulk dynamic response of a porous compact is not fully understood.

A recent investigation by Fredenburg et al [26] studied the static and dynamic response of three distinct morphology CeO_2 powders, with initial particle sizes differing by a factor of twenty. Under dynamic loading the consolidation responses

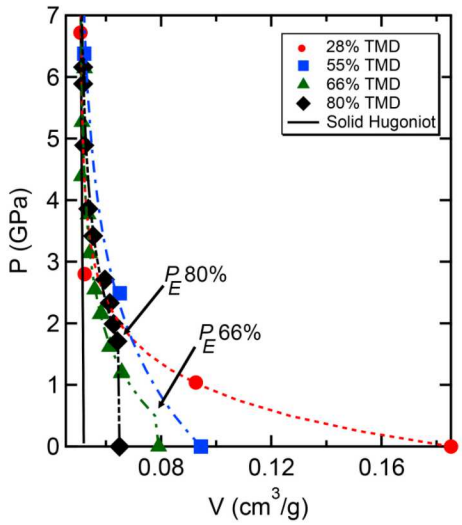

Fig. 9 Compaction data for porous tungsten plotted with P-α model fits from Eqn. (4) illustrating the transition from plastic to elastic plus plastic model response with decreasing initial porosity. Data for tungsten is taken from Bakanova et al [86], Boade [87], and Dandekar and Lamothe [88], with reported percentages of the theoretical maximum density (% TMD) calculated using ρ_0 = 19.257 g/cm^3 from the solid equation of state, SESAME 93540 [89].

of the three morphologies, following static compression to the same initial density state, were nearly indistinguishable within the reported uncertainties of the experiments, as shown in Fig. 10. This suggests that it is the initial porosity and the properties of the bulk material that have the greatest influence on the compaction response, and not the characteristics of the particle morphology. Support for this is offered by Grady [90], who proposed that the relatively low work of fracture leads to a turbulent-like separation of length scales under shock loading. In the case of CeO_2, this implies that the initial particle characteristics have little influence on the response because the particles can so readily fracture into smaller particles. However, Grady's argument does suggest that materials with vastly different particle sizes (orders of magnitude) can behave dissimilarly, but the variation in particle (or void) characteristics required to observe this difference is unknown and may be impractical to examine experimentally.

In contrast to the above argument that the dynamic compaction response is not influenced strongly by initial morphology, studies on granular and porous explosives as well as intermetallic and thermite mixtures have shown that initial characteristics of the particles and pores can have a significant effect on the energetic and reactive response. For example, coarse granular energetic materials such as HMX, TATB, PETN have been found to react more readily than those with fine particles, an observation that is typically attributed to the formation of hot spots under shock loading, which may originate from the closure of voids or the fracture and comminution of grains under dynamic loading. For intermetallic and thermite mixtures, reactivity

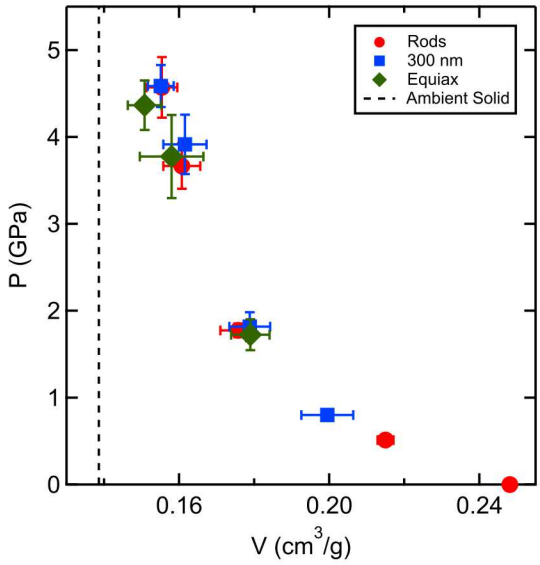

Fig. 10 Dynamic compaction response of three distinct morphologies of CeO_2 powders pressed to an initial porous density of $\rho_{00} = 4.03$ g/cm^3, or 56% TMD, illustrating nominally similar dynamic responses, regardless of morphology.

is favored by initial configurations that promote intimate mixing between the two constituents during shock loading. These types of systems have been covered extensively in the literature, and the interested reader is referred to Davison et al [91], Baer [65], and Eakins and Thadhani [21] for further details on their consolidation and energetic responses.

5 Outstanding Issues and Directions for Future Work

While significant progress has been made in the field of shock compaction in the past twenty years, there are still a number of outstanding issues related to (1) the experimental characterization of porous materials and targets, (2) the continuum and mesoscale modeling of these systems, and (3) theoretical considerations of their behavior. In this final section, the authors bring attention to several of these issues, and look forward to future research that can help move these areas forward.

Is the Compaction Response a Shock Hugoniot?

The analysis of shock experiments (and even simulations, in many cases) typically utilize the Rankine-Hugoniot jump conditions to calculate the stress/density/energy state behind the shock front, implicitly assuming that the compaction state reached lies on the porous Hugoniot corresponding to that initial density. Even for cases

where the shock wave has been shown to have reached a steady state [6], it is not entirely clear that the use of the jump conditions is appropriate. Such issues have been discussed for other types of materials by Krehl [92]. For example, the material passing through a shock front is treated as having instantaneously gone from its initial to final states by following a so-called Rayleigh line that connects the two states by a straight line in stress-volume space. However, in a porous material, or, indeed, any heterogeneous material, different material elements can have very different histories to the degree that no single material point may actually follow the Rayleigh line.

Another issue arises from the relatively long time scales needed to obtain thermal equilibrium when compared to those required for mechanical equilibrium. With this in mind, it is unlikely that thermodynamic equilibrium is achieved during the time it takes for the shock to transit the sample in the canonical compaction experiment, thus calling into question straightforward application of the jump conditions for initially porous materials. Despite these concerns, it seems likely that porous materials averaged over some suitable volume may indeed satisfy the Rankine-Hugoniot conditions. However, the limits of these approaches have not yet been defined, warranting further theoretical and numerical studies.

How are Dynamic and Static Responses Related?

While the focus of this chapter is on the shock response of porous materials, static experiments can also be used to characterize the compression response of initially porous materials. These static experiments are attractive from the standpoint of their relatively low cost with respect to dynamic experiments, allowing for the potential of more in-depth studies to be performed using static methods. While static studies are informative, there are a number of reasons to expect that the dynamic and static responses for a single material may be different. First, intrinsic rate dependence of the underlying material could play a role in the consolidation response in a manner similar to strength, where strain-rate dependent models may be required to capture the constitutive response, see for example Meyers [93]. More broadly, material deformation under shock loading is confined to much smaller regions, roughly the width of the shock front, as compared to deformation under quasi-static loads, which are applied to the bulk of the material. This distribution in stress, from local to global, is expected to significantly alter the densification response.

Unfortunately, relationships linking the static and dynamic compaction responses for porous materials are poorly understood, and experimental results can often contradict one another. In some cases [6, 94], the shock response was stiffer than the static response for all load levels. Zaretsky et al [95], on the other hand, found the two corresponded at the lowest stress levels measured but diverged for higher stresses. In contrast, studies of sand by Brown et al [5] found the dynamic and static compression response to be nearly equivalent, while [96] found the static response of aluminum foam was stiffer than the shock response. These differences likely stem, in part, from the difficulties associated with accurately executing and analyzing both static and dynamic compaction experiments. The ability to link densification responses under static and dynamic conditions has the potential to significantly

advance compaction theory toward the predictive, and should thus be given further attention.

How Should Heterogeneity Be Handled During Hugoniot Analysis?
Porous materials, especially foams and granular forms, will almost invariably have significant heterogeneity present on the scale of a few or many times the characteristic length of the grain or pore. Depending upon the scale and extent of heterogeneity, it has the potential to significantly affect the analysis and interpretation of experimental measurements that treat the material as a homogeneous continuum. Thus, it is incumbent upon experimentalists to minimize the heterogeneities that arise during sample preparation, or to be sure to include the heterogeneity in any analysis of experiments. In systems with high degrees of heterogeneities, where the heterogeneities themselves as a component of a porous system are important aspects of the system being studied, it may be necessary to characterize the initial samples through tomographic or radiographic techniques prior to performing dynamic experiments. For some material and target systems, this type of pre-shot characterization may be straightforward, but for others it may present significant challenges. However, if the role of heterogeneities are to be fully understood during the process of shock consolidation, then future work must be focused on the characterization and analysis of these features.

How Should Shock Compaction Be Modeled at the Continuum?
The continuum models for compaction discussed in Section 3.1 assume the compaction process is governed entirely by the hydrostatic pressure (mean stress) applied to the material. In contrast, so-called full stress models, such as those discussed by Banerjee and Brannon in this volume, consider the effect of the entire stress tensor on the material response. Since such full stress models generally require the calibration of a relatively large number of material constants compared to those based solely on pressure, the choice of implementing one model type over the other for modeling and simulation purposes may be material or application dependent. For materials with relatively low inherent strength, the hydrostatic approach may be sufficient for first, even second order accuracies of simulations under a broad range of loading configurations. However, for higher strength materials, calibration of continuum compaction models may require the inclusion of strength, whether it be a model of the full stress form or some other more simplified form.

What is the Role of Mesoscale Modeling?
In Section 3.2, some aspects of mesoscale modeling of porous materials were discussed. However, none of the approaches considered, Eulerian, Lagrangian, or molecular dynamics, are individually capable of modeling all of the mechanisms (fracture, large inelastic deformations, chemical reactions, etc.) and length and time scales (millimeters and microseconds or larger) that are important to compaction. Despite these limitations, mesoscale modeling approaches have proven useful for providing insights into the mechanical response of grains and pores under shock loading, as well as predicting specific aspects of the continuum response for a variety of porous materials classes. Improvements to the physics of mesoscale models are likely to occur in the relatively near-term future, as investigations into particle-level interactions under shock loading at advanced light sources, such as those dis-

cussed in the chapter by Jensen et al. become more common. As these experimental tools mature and become more widely used, they will likely have a profound impact on the fidelity of mesoscale modeling techniques.

6 Conclusion

In this chapter, the authors' intent was to present the physics of shock compaction from both a foundational and forward looking approach, while also capturing a segment of the areas in which this field is applied. In the first few sections, the foundations of experiment, diagnostics, and modeling approaches were covered, providing a snapshot in time of current capabilities. Following which, three specific applications of shock compaction physics were presented, ranging from planetary impacts to the formulation and penetration characteristics of munitions. In the final few sections, some of the unique features and observations of porous material responses to shock loading, as well as some of the major outstanding questions in the field were presented. From this mix of perspectives, it is hoped that the reader, and especially those that may be just beginning their careers in the field of shock compression science, finds motivation to push the limits of our current understanding of shock compaction physics for porous materials. While it is most definitely true that significant advancements have been made in this field over the years, significant advancements remain to be realized, and the authors look forward to the new discoveries that lie ahead.

7 Acknowledgements

Sandia National Laboratories is a multimission laboratory managed and operated by National Technology & Engineering Solutions of Sandia, LLC, a wholly owned subsidiary of Honeywell International Inc., for the U.S. Department of Energy's National Nuclear Security Administration under contract DE-NA0003525. Los Alamos National Laboratory is managed by Triad National Security, LLC for the U.S. Department of Energy's NNSA under contract number 89233218CNA000001.

References

[1] Grady D, Fenton G, Vogler T (2014) Equation of state for shock compression of distended solids. Journal of Physics: Conference Series 500(11):152007

[2] Fredenburg DA, Koller DD (2014) Interpreting the shock response of porous oxide systems. Journal of Physics: Conference Series 500(11):112025

[3] Nesterenko VF (2001) Dynamics of Heterogeneous Materials. Springer-Verlag, New York

[4] Fredenburg DA, Thadhani NN, Vogler TJ (2010) Shock consolidation of nanocrystalline 6061-T6 aluminum powders. Materials Science and Engineering A 527:3349-3357

[5] Brown JL, Vogler TJ, Grady DE, Reinhart WD, Chhabildas LC, Thornhill TF (2007) Dynamic compaction of sand. In: Elert M, Furnish MD, Chau R, Holmes N, Nguyen J (eds) Shock Compression of Condensed Matter-2007, AIP, New York, pp 1363–1366

[6] Vogler TJ, Lee MY, Grady DE (2007) Static and dynamic compaction of ceramic powders. International Journal of Solids and Structures 44:636-658

[7] Sheffield SA, Gustavsen RL, Anderson MU (1997) Shock loading of porous high explosives. In: Davison L, Horie Y, Shahinpoor M (eds) High-Pressure Shock Compression of Solids IV: Response of Highly Porous Solids to Shock Loading, Springer-Verlag, N.Y., pp 23–61

[8] Trott WM, Baer MR, Castaeda JN, Chhabildas LC, Asay JR (2007) Investigation of the mesoscopic scale response of low-density pressings of granular sugar under impact. Journal of Applied Physics 101:024917

[9] Yang R, Zou R, Yu A (2003) Effect of material properties on the packing of fine particles. Journal of Applied Physics 94:3025-3034

[10] Fredenburg DA, Koller DD, Rigg PA, Scharff RJ (2013) High-fidelity Hugoniot analysis of porous materials. Review of Scientific Instruments 84:013903

[11] Borg JP, Vogler TJ (2008) Mesoscale calculations of the dynamic behavior of a granular ceramic. International Journal of Solids and Structures 45:1676-1696

[12] Benson DJ (1995) The calculation of the shock velocity - particle velocity relationship for a copper powder by direct numerical simulation. Wave Motion 21:85-99

[13] Schumaker MG, Kennedy G, Thadhani NN, Hankin M, Stewart ST, Borg JP (2017) Stress and temperature distributions of individual particles in a shock wave propagating through dry and wet sand mixtures. In: AIP Conference Proceedings 1793, American Institute of Physics, p 120016

[14] Jaeger HM (2005) Sand, jams and jets. Physics World 18:34-39

[15] Elliot NE, Staudhammer KP (1992) Effect of internal gas pressure on the shock consolidation of 304 stainless steel powders, Marcel Dekker, New York, pp 371–381

[16] McQueen RG, Marsh SP, Taylor JW, Fritz JN, Carter WJ (1970) The equation of state of solids from shock wave studies. In: Kinslow R (ed) High-Velocity Impact Phenomena, Academic Press, New York, pp 293–417

[17] Yiannakopoulos G (1990) A review of manganin gauge technology for measurements in the gigapascal range. Tech. Rep. MRL-TR-90-5, Materials Research Labs Ascot Vale, Australia
[18] Bauer F (1982) Behavior of ferroelectric ceramics and PVF2 polymers under shock loading. In: Nellis WJ, Seaman L, Graham RA (eds) Shock Waves in Condensed Matter - 1981, AIP, New York, pp 251–266
[19] Barker LM, Hollenbach RE (1972) Laser interferometry for measuring high velocities for any reflecting surface. Journal of Applied Physics 43:4669-4675
[20] Strand OT, Goosman DR, Martinez C, Whitworth TL, Kuhlow WW (2006) Compact system for high-speed velocimetry using heterodyne techniques. Review of Scientific Instruments 77:083108
[21] Eakins DE, Thadhani NN (2009) Shock compression of reactive powder mixtures. International Materials Reviews 54:181-213
[22] Borg JP, Chapman DJ, Tsembelis K, Proud WG, Cogar JR (2005) Dynamic compaction of porous silica powder. Journal of Applied Physics 98:073509
[23] Dai C, Eakins DE, Thadhani NN (2007) On the applicability of analytical models to predict Hugoniot of nano-sized powder compacts. In: Elert M, Furnish MD, Chau R, Holmes N, Nguyen J (eds) Shock Compression of Condensed Matter-2007, AIP, New York, pp 35–38
[24] Razorenov SV, Kanel GI, Baumung K, Bluhm HJ (2002) elastic limit and spall strength of aluminum and copper single crystals over a wide range of strain rates and temperatures. In: Shock Compression of Condensed Matter - 2001, American Institute of Physics, pp 503–506
[25] Barker LM, Hollenbach RE (1974) Shock wave study of the alpha to epsilon phase transition in iron. Journal of Applied Physics 45:4872
[26] Fredenburg DA, Koller DD, Coe JD, Kiyanda CB (2014) The influence of morphology on the low- and high-strain-rate compaction response of CeO_2 powders. Journal of Applied Physics 115:123511
[27] Barker LM, Hollenbach RE (1970) Shock-wave studies of PMMA, fused silica, and sapphire. Journal of Applied Physics 41:4208-4226
[28] Baer MR, Trott WM (2004) Mesoscale studies of shock loaded tin sphere lattices. In: Furnish MD, Gupta YM, Forbes JW (eds) Shock Compression of Condensed Matter, American Institute of Physics, pp 517–520
[29] Mitchell AC, Nellis WJ (1981) Shock compression of aluminum, copper, and tantalum. Journal of Applied Physics 52:3363-3374
[30] Root S, Haill TA, Lane JMD, Thompson AP, Grest GS, Schroen DG, Mattsson TR (2013) Shock compression of hydrocarbon foam to 200 GPa: experiments, atomistic simulations, and mesoscale hydrodynamic modeling. Journal of Applied Physics 114:103502
[31] Boade RR (1968) Compression of porous copper by shock waves. Journal of Applied Physics 39:5693-5702
[32] Tang Z, Aidun JB (2009) Combined compression and shear plane waves. In: Horie Y (ed) Shock Wave Science and Technology Reference Library, vol 3, Springer, Berlin, pp 109–167

[33] Sairam S, Clifton RJ (1994) Pressure-shear impact investigation of dynamic fragmentation and flow of ceramics. In: Gilat A (ed) Mechanical Testing of Ceramics and Ceramic Composites, AMD Vol. 197, ASME, New York, pp 23–40

[34] Vogler TJ, Alexander CS, Thornhill TF, Reinhart WD (2011) Pressure-shear experiments on granular materials. Report SAND2011-6700, Sandia National Laboratories

[35] LaJeunesse JW (2018) Dynamic behavior of granular earth materials subjected to pressure-shear loading. Ph.d. thesis, Marquette University, Department of Mechanical Engineering

[36] Sakharov AD, Zaidel RM, Mineev VN, Oleinik AG (1965) Experimental investigation of the stability of shock waves and the mechanical properties of substances at high pressures and temperatures. Soviet Physics JETP 9:1091-1094

[37] Vogler TJ (2015) Shock wave perturbation decay in granular materials. Journal of the Dynamic Behavior of Materials 1:370-387

[38] Carton EP, Verbeek HJ, Stuivinga M, Schoonman J (1997) Dynamic compaction of powders by an oblique detonation wave in the cylindrical configuration. Journal of Applied Physics 81:3038-3045

[39] Thadhani NN (1988) Shock compression of powders. Advanced Materials and Manufacturing Processes 3:493-549

[40] Jin ZQ, Thadhani NN, McGill M, Ding Y, Wang ZL, Chen M, Zeng H, Chakka VM, Liu JP (2005) Explosive shock processing of $Pr_2Fe_{14}B/\alpha$-Fe exchange-coupled nanocomposite bulk magnets. Journal of Materials Research 20:599-609

[41] Sethi G, Myers NS, German RM (2008) An overview of dynamic compaction in powder metallurgy. International Materials Reviews 53:219-234

[42] Nesterenko VF, Meyers MA, Chen HC (1996) Shear localization in high-strain-rate deformation of granular alumina. Acta Materialia 44:2017-2026

[43] Shih CJ, Meyers MA, Nesterenko VF (1998) High-strain-rate deformation of granular silicon carbide. Acta Materialia 46:4037-4065

[44] Fenton G, Caipen T, Daehn G, Vogler T, Grady D (2009) Shock-less high rate compaction of porous brittle materials. In: Elert ML, Buttler WT, Furnish MD, Anderson WW, Proud WG (eds) Shock Compression of Condensed Matter 2009, AIP, pp 1337–1340

[45] Herrmann W (1969) Constitutive equations for the dynamic compaction of ductile porous materials. Journal of Applied Physics 40:2490-2499

[46] Carroll M, Holt AC (1972) Suggested modification of the p-alpha model for porous materials. Journal of Applied Physics 43:759-761

[47] Butcher BM, Karnes CH (1969) Dynamic compaction of porous iron. Journal of Applied Physics 40:2967-2976

[48] Carroll M, Holt AC (1974) Shock-wave compaction of porous aluminum. Journal of Applied Physics 45:3864-3875

[49] Fredenburg DA, Thadhani NN (2013) On the applicability of the p-alpha and p-lambda models to describe the dynamic compaction response of highly heterogeneous powder mixtures. Journal of Applied Physics 113:043507
[50] Boade RR (1970) Principal Hugoniot, second-shock Hugoniot, and release behavior of pressed copper powder. Journal of Applied Physics 41:4542-4551
[51] Grady DE, Winfree NA, Kerley GI, Wilson LT, Kuhns LD (2000) Computational modeling and wave propagation in media with inelastic deforming microstructure. Journal de Physique IV 10:15-20
[52] Grady DE, Winfree NA (2001) A computational model for polyurethane foam. In: Staudhammer KP, Murr LE, Meyers MA (eds) Fundamental Issues and Applications of Shock-Wave and High-Strain-Rate Phenomena, Elsevier, New York, pp 485–491
[53] Fenton G, Grady D, Vogler T (2015) Shock compression modeling of distended mixtures. Journal of Dynamic Behavior of Materials 1:103
[54] Collins GS, Melosh HJ, Wunneman K (2011) Improvements to the ε-α porous compaction model for simulating impacts into high-porosity solar system objects. International Journal of Imoact Engineering 38:434-439
[55] Wunnemann K, Collins GS, Melosh HJ (2006) A strain-based porosity model for use in hydrocode simulations of impacts and implications for transient crater growth in porous targets. Icarus 180:514-527
[56] Bland PA, Collins GS, Davison TM, Abreu NM, Ciesla FJ, Muxworthy AR, Moore J (2014) Pressure-temperature evolution of primordial solar systems during impact-induced compaction. Nature Communications 5:5451
[57] Davison TM, Collins GS, Bland PA (2016) Mesoscale modeling of impact compaction of primitive solar system models. The Astrophysical Journal 821:68
[58] Benson DJ (1997) The numerical simulation of the dynamic compaction of powders. In: Davison L, Horie Y, Shahinpoor M (eds) High-Pressure Shock Compression of Solids IV: Response of Highly Porous Solids to Shock Loading, Springer-Verlag, N.Y., pp 233–255
[59] Borg JP, Vogler TJ (2008) Mesoscale simulations of a dart penetrating sand. International Journal of Impact Engineering 35:1435-1440
[60] Dwivedi SK, Teeter RD, Felice CW, Gupta YM (2008) Two dimensional mesoscale simulations of projectile instability during penetration in dry sand. Journal of Applied Physics 104:083502
[61] Homel MA, Herbold EB (2017) On mesoscale methods to enhance full-stress continuum modeling of porous compaction. In: Chau R, Germann T, Oleynik I, Peiris S, Ravelo R, Sewell T (eds) Shock Compression of Condensed Matter - 2015, AIP Publishing, vol 1793, p 080010
[62] Borg JP, Vogler TJ (2013) Rapid compaction of granular materials: characterizing two and three-dimensional mesoscale simulations. Shock Waves 23:153-176
[63] Lajeunesse JW, Hankin M, Kennedy GB, Spaulding DK, Schumaker MG, Neel CH, Borg JP, Stewart ST, Thadhani NN (2017) Dynamic response of dry and water-saturated sand systems. Journal of Applied Physics 112:015901

[64] Borg JP, Vogler TJ (2009) Aspects of simulating the dynamic compaction of a granular ceramic. Modelling and Simulation in Materials Science and Engineering 17:045003
[65] Baer MR (2007) Mesoscale modeling of shocks in heterogeneous reactive materials. In: Horie Y (ed) Shock Wave Science and Technology Reference Library, Springer, Heidelberg, pp 321–356
[66] Benson DJ, Conley P (1999) Eulerian finite-element simulations of experimentally acquired hmx microstructures. Modelling and Simulation in Materials Science and Engineering 7:333-354
[67] Eakins D, Thadhani NN (2007) Discrete particle simulation of shock wave propagation in a binary Ni+Al powder mixture. Journal of Applied Physics 101:043508
[68] McGlaun JM, Thompson SL, Elrick MG (1990) CTH: a three-dimensional shock wave physics code. International Journal of Impact Engineering 10:351-360
[69] Williamson RL (1990) Parametric studies of dynamic powder consolidation using a particle-level numerical model. Journal of Applied Physics 68:1287-1296
[70] Derrick JG, LaJeunesse JW, Davison TM, Borg JP, Collins GS (2018) Mesoscale simulations of shock compaction of a granular ceramic: effects of mesostructure and mixed-cell strength treatment. Modelling and Simulation in Materials Science and Engineering 26:035009
[71] Borg JP, Maines WR, Chhabildas LC (2014) Equation of state and isentropic release of aluminum foam and polyvinylidene fluoride systems. Journal of Applied Physics 115:213515
[72] Dwivedi SK, Pei L, Teeter RD (2015) Two-dimensional mesoscale simulations of shock response of dry sand. Journal of Applied Physics 117:085902
[73] Xi CQ, Li QM (2017) Meso-scale mechanism of compaction shock propagation in cellular materials. International Journal of Impact Engineering 109:321-334
[74] Labanda NA, Giusti SM, Luccioni BM (2018) Meso-scale fracture simulation using an augmented Lagrangian approach. International Journal of Damage Mechanics 27:138-175
[75] Gunkelmann N, Rosandi Y, Ruestes CJ, Bringa EM, Urbassek HM (2016) Compaction and plasticity in nanofoams induced by shock waves: a molecular dynamics study. Computational Materials Science 119:27-32
[76] Banlusan K, Strachan A (2016) Shockwave energy dissipation in metal-organic framework MOF-5. Journal of Physical Chemistry C 120:12463-12471
[77] Cheruka MJ, Germann TC, Kober EM, Strachan A (2014) Shock loading of granular Ni/Al composites. Part I: mechanics of loading. The Journal of Physical Chemistry C 118:26377-26386
[78] Lane JMD, Thompson AP, Vogler TJ (2014) Enhanced densification under shock compression in porous silicon. Physical Review B 90:134311

[79] Brar NS, Rosenberg Z, Bless SJ (1992) Applying steinberg's model to the Hugoniot elastic limit of porous boron carbide specimens. In: Schmidt SC, Dick RD, Forbes JW, Tasker DG (eds) Shock Compression of Condensed Matter, North-Holland, pp 467–470
[80] Neal WD, Chapman DJ, Proud WG (2012) Shock-wave stability in quasi-mono-disperse granular materials. The European Physical Journal Applied Physics 57:31001
[81] Tong W, Ravichandran G (1997) Recent developments in modeling shock compression of porous materials. In: Davison L, Horie Y, Shahinpoor M (eds) High-Pressure Shock Compression of Solids IV: Response of Highly Porous Solids to Shock Loading, Springer-Verlag, N.Y., pp 177–203
[82] Swegle JW, Grady DE (1985) Shock viscosity and the prediction of shock wave rise times. Journal of Applied Physics 58:692-701
[83] Zhuang S, Ravichandran G, Grady DE (2003) An experimental investigation of shock wave propagation in periodically layered composites. Journal of the Mechanics and Physics of Solids 51:245-265
[84] Vogler TJ, Borg JP, Grady DE (2012) On the scaling of steady structured waves in heterogeneous materials. Journal of Applied Physics 112:123507
[85] Zeldovich YaB, Raizer YuP (2002) Physics of shock waves and high-temperature hydrodynamic phenomena. Dover Publications, Inc., Mineola, NY
[86] Bakanova AA, Dudoladov IP, Sutulov YN (1974) Shock compressibility of porous tungsten, molybdenum, copper, and aluminum in the low pressure domain. Journal of Applied Mechanics and Technical Physics 15:241-245
[87] Boade RR (1969) Dynamic compression of porous tungsten. Journal of Applied Physics 40:3781-3785
[88] Dandekar DP, Lamothe RM (1977) Behavior of porous tungsten under shock compression at room temperature. Journal of Applied Physics 48:2871-2897
[89] Crockett S (2017) Sesame equation of state 93540. SESAME Database
[90] Grady DE (2010) Length scales and size distributions in dynamic fragmentation. International Journal of Fracture 163:85-99
[91] Davison L, Horie Y, Shahinpoor M (eds) (1997) High-pressure shock compression of solids IV: response of highly porous solids to shock loading. Springer, New York
[92] Krehl POK (2015) The classical Rankine-Hugoniot jump conditions, an important cornerstone of modern shock wave physics: ideal assumptions vs. reality. The European Physical Journal H 40:159-204
[93] Meyers MA (1994) Dynamic Behavior of Materials. John WIley & Sons, New York
[94] Lagunov VA, Stepanov VA (1963) Measurements of the dynamic compressibility of sand. Zhurnal Prikladnoi Mekhaniki i Tehknicheskoi Fiziki 4:88-96
[95] Zaretsky E, Asaf Z, Ran E, Aizik F (2012) Impact response of high density flexible polyurethane foam. International Journal of Impact Engineering 39:1-7

[96] Barnes AT, Ravi-Chandar K, Kyriakides S, Gaitanaros S (2014) Dynamic crushing of aluminum foams: Part I - experiments. International Journal of Solids and Structures 51:1631-1645